Available online at www.sciencedirect.com
ScienceDirect
Journal of Power Sources 172 (2007) 742–748
JOURNAL OF POWER SOURCES
www.elsevier.com/locate/jpowsour

Development of LSM-based cathodes for solid oxide fuel cells based on YSZ films

Kongfa Chen [a], Zhe Lü [a,*], Xiangjun Chen [b], Na Ai [a], Xiqiang Huang [a], Xiaobo Du [c], Wenhui Su [a,c,d]

[a] *Center for Condensed Matter Science and Technology, Harbin Institute of Technology, Harbin 150001, China*
[b] *Division for Theoretical Physics, Harbin Institute of Technology, Harbin 150001, China*
[c] *Department of Condensed Matter, Jilin University, Changchun 130022, China*
[d] *International Center for Material Physics, Academia, Shenyang 110015, China*

Received 22 April 2007; received in revised form 12 May 2007; accepted 15 May 2007
Available online 21 May 2007

Abstract

In an attempt to achieve desirable cell performance, the effects of $La_{0.7}Sr_{0.3}MnO_3$ (LSM)-based cathodes on the anode-supported solid oxide fuel cells (SOFCs) were investigated in the present study. Three types of cathodes were fabricated on the anode-supported yttria-stabilized zirconia (YSZ) thin films to constitute several single cells, i.e., pure LSM cathode, LSM/YSZ composite by solid mixing, LSM/$Sm_{0.2}Ce_{0.8}O_{1.9}$ (SDC) composite by the ion-impregnation process. Among the three single cells, the highest cell output performance 1.25 W cm^{-2} at 800 °C, was achieved by the cell using LSM/SDC cathode when the cathode was exposed to the stationary air. Whereas, the most considerable cell performance of 2.32 W cm^{-2} was derived from the cell with LSM/YSZ cathode, using 100 ml min^{-1} oxygen flow as the oxidant. At reduced temperatures down to 700 °C, the LSM/SDC cathode was the most suitable cathode for zirconia-based electrolyte SOFC in the present study. The variation in the cell performances was attributed to the mutual effects between the gas diffusing rate and three-phase boundary length of the cathode.
© 2007 Elsevier B.V. All rights reserved.

Keywords: SOFC; LSM; YSZ film; TPB; Porosity

1. Introduction

At present, the most common materials for solid oxide fuel cells (SOFCs) are oxide ion-conducting yttria-stabilized zirconia (YSZ) for the electrolyte, strontium-doped lanthanum manganite (LSM) for the cathode and nickel/YSZ for the anode [1]. The development of anode-supported YSZ thin film fabrication processes has largely lowered the ohmic resistance [2–4]. It results in the reduction of the operating temperature from ~1000 °C to intermediate temperature range (600–800 °C). Further reduction in the operating temperature is dependant on the decrease in the electrode polarization resistances. It is known that the polarization resistance of the anode is much lower than that of the cathode [5,6], due to much faster electrochemical oxidation reaction of the hydrogen at the anode side. Eventually, the high cathode polarization loss turns to be the dominant factor limiting the promotion of the cell performance at reduced temperatures.

LSM cathode is regarded as one of the most promising cathode materials for high temperature SOFCs because of its excellent electrochemical performance, thermal and chemical stability and relatively good compatibility with YSZ [7]. Unfortunately, LSM is limited at reduced temperatures as result of its low oxygen ion conductivity and high activation energy for oxygen dissociation [8]. It is found that the addition of an electrolyte component to the LSM in the formation of the composite cathodes dramatically enhances the cathode electrochemical performance [5,9]. It is attributed to the extension of the three-phase boundary (TPB) areas from the electrolyte/cathode interface deep into the bulk cathode.

In the literatures [9–12], the electrolyte phase in the composite cathodes was YSZ or doped-ceria (DCO). They have their own advantages and disadvantages. For instance, YSZ compo-

* Corresponding author. Tel.: +86 451 86418420; fax: +86 451 86412828.
E-mail addresses: explorer_081@163.com (K. Chen), lvzhe@hit.edu.cn (Z. Lü).

0378-7753/$ – see front matter © 2007 Elsevier B.V. All rights reserved.
doi:10.1016/j.jpowsour.2007.05.035

nent matches well with the electrolyte material, but the ionic conductivity is relatively low; DCO possesses much higher ionic conductivity than YSZ, but the thermal expansion coefficient (TEC) is mismatched with the YSZ electrolyte. In addition, the comparisons of the LSM/DCO and LSM/YSZ cathodes were usually performed using a three-electrode method at open-circuit conditions. Few reports have focused on the applications of the two cathodes in practical fuel cells in one paper. This, to some extent, can directly show the evidence of the usefulness of the cathodes.

In the present study, LSM, LSM/YSZ and LSM/$Sm_{0.2}Ce_{0.8}O_{1.9}$ (SDC) cathodes were fabricated onto the anode-supported YSZ films, respectively. The effects of the three cathodes on the cell performance are presented and discussed.

2. Experimental

NiO was synthesized by the precipitation method, using $Ni(NO_3)_2{\cdot}6H_2O$ (Analytical reagent, A.R.) and ammonia (A.R.) as the raw materials. In the green anode powder, NiO, YSZ (TZ-8Y) and flour were mixed in the weight ratio of 5:5:2.2. The compacted anode pellets were calcined at 1000 °C for 2 h. Thirteen micrometer thick dense YSZ thin films were deposited onto the NiO–YSZ substrates by slurry spin coating, as reported previously [3]. The anode/YSZ film bi-layers were then co-fired at 1400 °C for 2 h.

LSM ($La_{0.7}Sr_{0.3}MnO_3$) powder was synthesized by the Pechini method, using $La(NO_3)_3{\cdot}6H_2O$ (A.R.), $Sr(NO_3)_2$ (A.R.), $Mn(NO_3)_2$ (A.R.) and citric acid monohydrate (A.R.) as the raw materials. The resultant powder was calcined at 1000 °C and ball-milled. Three types of LSM-based cathodes were fabricated: pure LSM cathode, LSM/YSZ composite cathode and $Sm_{0.2}Ce_{0.8}O_{1.9}$ (SDC)/LSM composite cathodes. The LSM and solid-mixed LSM/YSZ composite were mixed with a binder to form pastes and coated onto the sintered YSZ films, respectively. The sintered temperatures were 1100 and 1200 °C, respectively. LSM/SDC cathodes were fabricated upon the $Sm_{0.2}Ce_{0.8}(NO_3)_x$ solution impregnation of the sintered pure LSM cathode (1100 °C), and heat-treated at 850 °C. The impregnation–calcination process was repeated for several cycles to obtain a desirable LSM/SDC composition. In our previous work, the cell with LSM/SDC composite made by solid mixing achieved relatively poor performance. It is likely caused by the poor contact at the electrolyte/cathode interface due to the mismatched thermal expansion coefficient between the two electrolyte materials and the smooth surface of the YSZ film [13]. On the other hand, the impregnation process is an effective way to fabricate LSM/SDC composite [14]. That is the reason why LSM/SDC cathode is fabricated by impregnation method instead of solid mixing process. The details of the samples were listed in Table 1.

The cell was measured with a four-probe method individually under the similar conditions. The cell was heating up gradually in a furnace, and the anode was reduced in situ at 800 °C for 15 min, followed by the measurement of the initial I–V characteristic. Then the stable testing of the newly fabricated cell was conducted under a constant current at around maximum power density and the cell voltage was recorded. When the recorded cell voltage was stable, the temperature was lowered to 600 °C. And the measurement of the cell performance was subsequently carried out from 600 to 800 °C at an interval of 100 °C. Hydrogen was used as fuel and stationary air as oxidant. In some cases, oxygen flow supplied with an alumina tube was introduced at the cathode side in the ambient air as an additional oxidant. Electrochemical characteristics were performed with an electrochemical interface SI 1287 and impedance/gain analyzer SI 1260 (Solartron Instruments, Hampshire, UK). The impedance spectra were measured in the frequency range from 0.1 to 91 kHz under open-circuit conditions with an AC signal amplitude of 10 mV.

Table 1
Cathode characteristics of the cells

Sample	Composition	LSM ratio (wt%)	Fabrication method
Cell-1	Pure LSM	100	Solid mixing
Cell-2	LSM/YSZ	50	Solid mixing
Cell-3	LSM/SDC	58	Ion-impregnation

3. Results and discussion

3.1. Cell microstructures

Fig. 1 shows the microstructures of the fractured cells with different cathodes after electrochemical testing, i.e., pure LSM, LSM/YSZ and LSM/SDC cathodes, respectively. All of the cathodes bond well with the electrolyte films. The particles in the respective cathode contact well with each other. The cathode particle sizes in Fig. 1a are smaller than those in Fig. 1b and the porosity of the cathode in Fig. 1a seems larger than that in Fig. 1b, due to 100 °C lower sintering temperature. As reported by Murray [9], for a given electrode composition, the impedance measured showed no detectable difference between samples sintered at different temperatures. So the performance of LSM/YSZ sintered 1200 °C is comparable with that sintered at 1100 °C, which can be used to compare with the pure LSM cathode sintered at 1100 °C. In addition, the relatively high sintering temperature can result in well-bonded particles so that the LSM electronic and YSZ ionic conducting paths can be successfully formed, respectively. The LSM/SDC cathode in Fig. 1c was fabricated upon the impregnation of fine SDC particles into the LSM structures (see Fig. 1a), so the microstructure appears somewhat dense and lack of porosity. One the other hand, the dense morphology also demonstrates the formation of a continuous network of SDC conducting path. The contact of the cathode and YSZ film at the interface is intimate. The pores and gaps in the interface have been filled up by the SDC particles, which be beneficial to fast charge transport through the interface. The YSZ film (~13 μm thick) in Fig. 1d appears uniform and dense, bonding well to the porous Ni/YSZ anode.

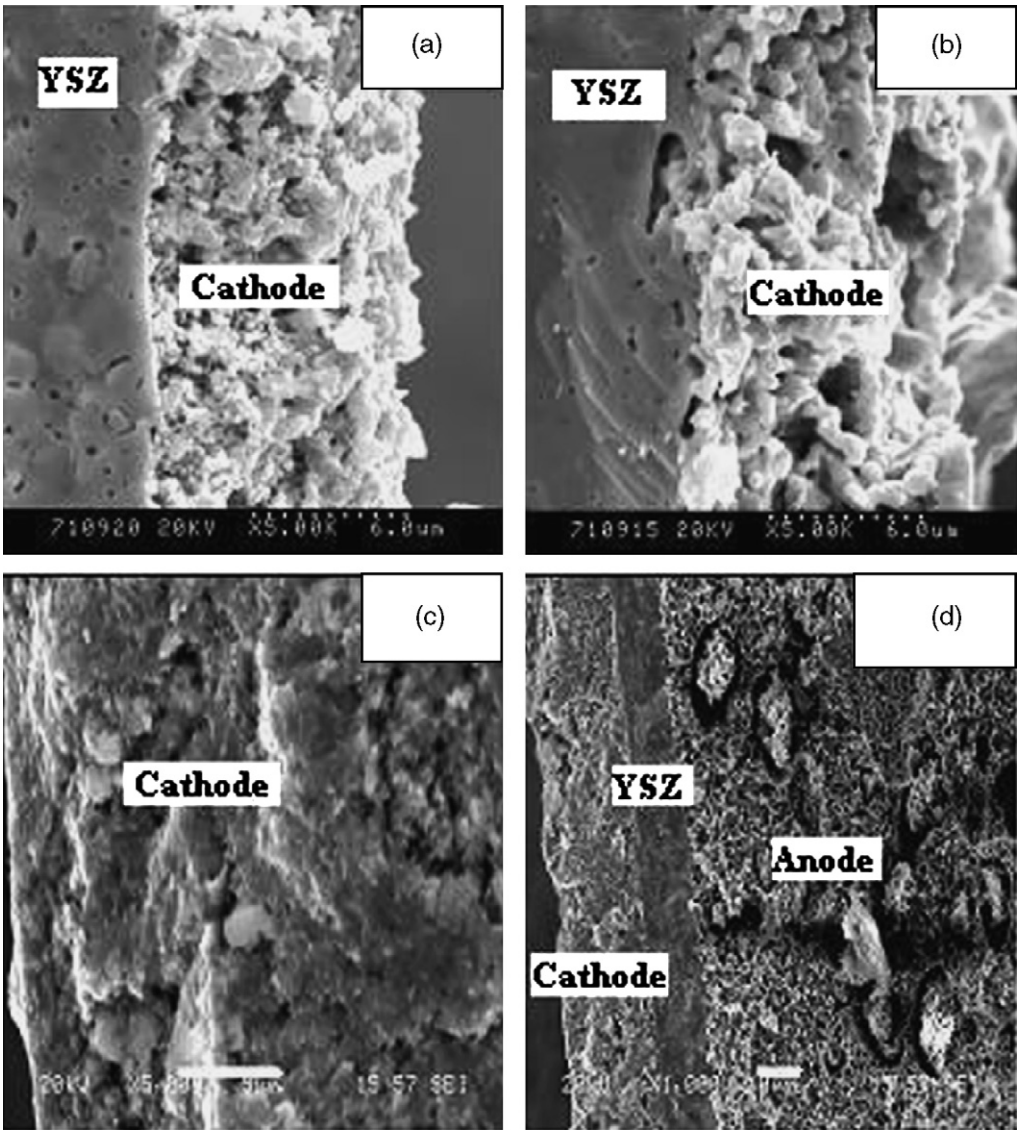

Fig. 1. Microstructures of the fractured cells after electrochemical testing: (a) Cell-1, (b) Cell-2, (c) and (d) Cell-3 (The scale bars are 6.0, 6.0, 5.0 and 10 μm in Fig. 1a, b, c and d, respectively.).

3.2. Cell performance with the stationary air as oxidant

Shown in Fig. 2 are the electrochemical characteristics of the three single cells at 800 °C. Maximum power densities (MPDs) of Cell-1, Cell-2 and Cell-3 are 0.82, 1.10, 1.25 W cm^{-2}, respectively. The anodes and the YSZ films were fabricated with the same processes and the cells were tested with the same conditions, so the difference among the cells should be attributed to the contribution of the different cathodes. It is surprising that relatively desirable cell output performance has been achieved by Cell-1 with the pure LSM at intermediate temperature. It should be due to the extension of TPB from the LSM cathode/YSZ electrolyte interface to the LSM surface as a result of the formation and propagation of oxygen ion vacancies when LSM is under sufficient cathodic polarization [15]. The result in the present study is superior to the literatures with the same pure LSM cathode [16], LSM/YSZ cathode [4] and even LSM/Pt cathode [17]. It is likely due to the optimized cathode microstructure as well

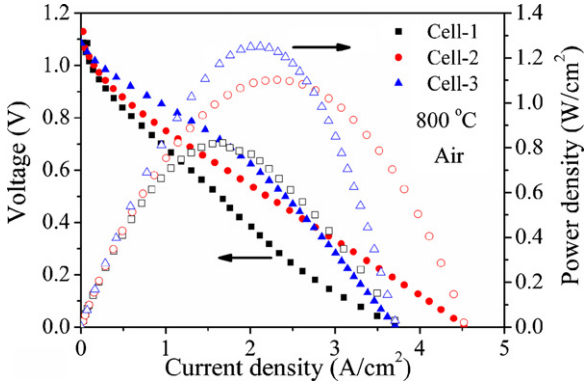

Fig. 2. Electrochemical characteristics of the cells with the cathode exposed to the stationary air at 800 °C.

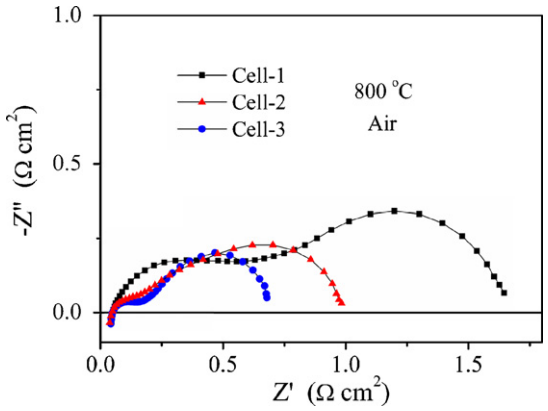

Fig. 3. Cell impedance spectra under open-circuit conditions at 800 °C.

as the optimized fabrication process of the anode/YSZ film bilayer. With the addition of the YSZ ionic conducting phase in the LSM structure, the cell performance of Cell-2 is largely promoted by 34% compared with that of Cell-1. It is due to the improved cathode performance, resulting from the extension of the TPB areas from the electrolyte/cathode interface deep into the bulk cathode. As can be observed, no detectable electrode concentration polarization phenomenon usually related to the negative curvature of the I–V characteristics can be observed in Cell-1 and Cell-2. It indicates that the difference in the sintering temperature of the two cathodes has no obvious influence in affecting the cathode gas transport property. By substituting YSZ (0.04 S cm^{-1} at 800 °C [6]) with the high ionic conducting SDC phase (0.1 S cm^{-1} at 800 °C [18]) in the LSM/SDC cathode, the MPD of the single cell is further enhanced, e.g., MPD of Cell-3 is 53 and 14% higher than that of Cell-1 and Cell-2, respectively. Similarly, the promotion in Cell-3 relative to Cell-1 arises from the extended TPB sites in the cathode. Also, the higher ionic conductivity and higher oxygen surface exchange coefficient of SDC than those of YSZ are suggested as the two main factors aiding electrode processes [9]. Furthermore, the special redox properties of Ce^{4+} and Ce^{3+} can facilitate the surface diffusion and charge transfer processes [19]. These are the reasons why the Cell-3 performance is higher than Cell-2. Note that the Cell-3 performance is practically limited by the serious cathode concentration polarization at high current density region, which is corresponded to limited gas transport rate through the relatively dense cathode (see Fig. 1c and d).

Fig. 3 illustrates cell impedance spectra under open-circuit conditions when the cathodes were exposed to the stationary air. As can be observed, the high frequency intercept of the impedance spectra, namely, the ohmic resistances are approximately similar. Due to the negligible anode polarization resistance (R_a) at low current density [5,6], the difference between the high and low frequency intercepts, i.e., electrode interfacial resistance can be regarded as the cathode polarization resistance (R_c). And the decreased R_c value demonstrates the continuously improved cathode electrochemical performance of the LSM, LSM/YSZ and LSM/SDC cathodes, in good accordance with the cell output performance in Fig. 2.

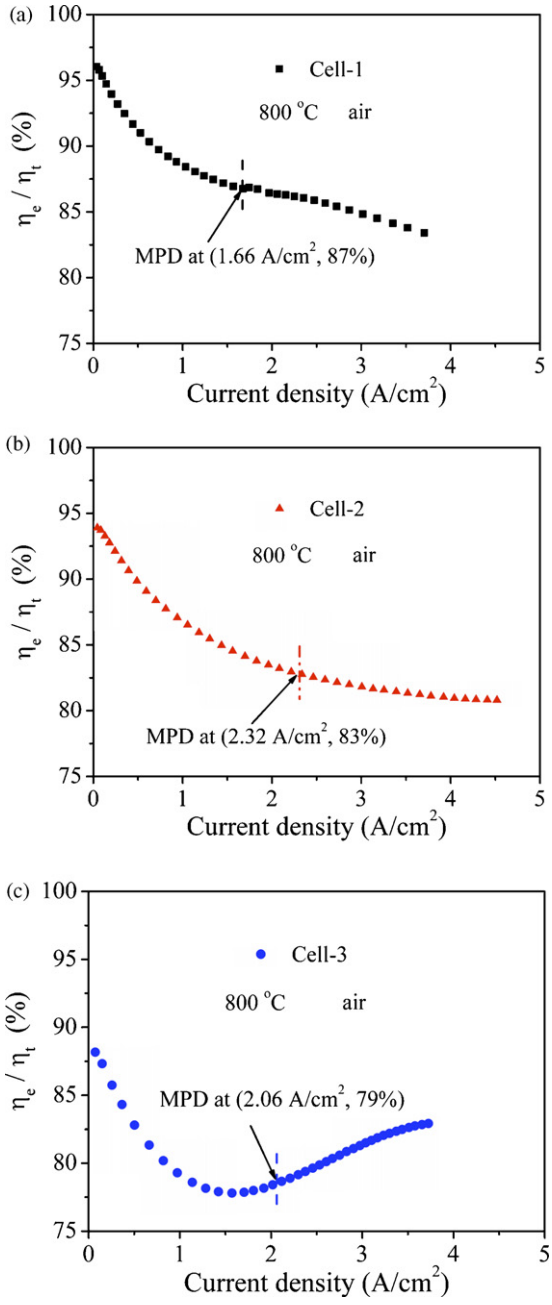

Fig. 4. The ratio of electrode polarization loss in the total cell polarization loss as a function of current density at 800 °C, using air as the oxidant: (a) Cell-1, (b) Cell-2 and (c) Cell-3.

It is noted that the impedance spectra at open-circuit can only reflect the cell performance in the case of very low current density. The total polarization resistance under current loading correlates well with the power density of the cell under that loading [20]. So the distribution of the ratio of the electrode polarization loss (η_e), i.e., cathode polarization loss in the total polarization loss ($\eta_t = \eta_e + iR_{ohm}$, set $\eta_e\% = \eta_e/\eta_t$) with the current density can be used to evaluate the cell performance, as illustrated in Fig. 4. The η_e% values of Cell-1 and Cell-2 are gradually decreased with the current density. What is different is that the η_e% value of Cell-3 decreases rapidly with the current density at the initial stage, and begins to increase

after it reaches a minimum at 1.60 A cm^{-2}. The minimum point in the η_e% curve indicates that when the current density is higher than 1.60 A cm^{-2}, mass transfer process (rds) mainly limits the promotion of the cell performance. As also marked in Fig. 4, the η_e% values at MPD are 87, 83 and 78% for the three cells, respectively, demonstrating that the high cathode electrode polarization loss at intermediate temperature is still the predominant factor limiting the cell performance. So it is predicted that any decrease in the cathode overpotential will bring forth a pronounced increase in the cell performance. The MPD of Cell-3 occurs at the point where the contribution of concentration polarization is increasing. As expected, a higher cell output with the LSM/SDC cathode at 800 °C can be achieved probably if the cathode porosity is increased while the cathode composition of LSM and SDC is maintained. Or the stationary air could be altered by the flowing air, which would effectively suppress the limitation of the gases movement in and out of the active reaction sites through the fine pores.

3.3. Cell performance with oxygen as an additional oxidant

In an attempt to further improve the cell performance, 100 ml min^{-1} oxygen flow was introduced at the cathode side as an additional oxidant, and the cell performances are shown in Fig. 5. The cell outputs are substantially promoted with the oxygen oxidant, e.g., the MPDs are 1.56, 2.32 and 1.71 W cm^{-2} for Cell-1, Cell-2 and Cell-3 at 800 °C, respectively. The MPDs are 90, 110 and 37% higher than those with the air oxidant for Cell-1, Cell-2 and Cell-3, respectively. The MPD of Cell-2 is better than the high cell performance (2.24 W cm^{-2} at 800 °C) with LSM/Sc_2O_3-stabilized ZrO_2 co-doped CeO_2 (ScSZ) cathode [19]. The dramatic promotion in the cell performance, typically Cell-2 well implies that gas conditions at the cathode side as well as the cathode microstructure and porosity play a significant role in determining the cell performance.

Open-circuit voltages (OCVs) of the cells with the oxygen oxidant are slightly increased compared with those with air oxidant, e.g., from 1.12 to 1.13 V for Cell-1. According to the Nernst

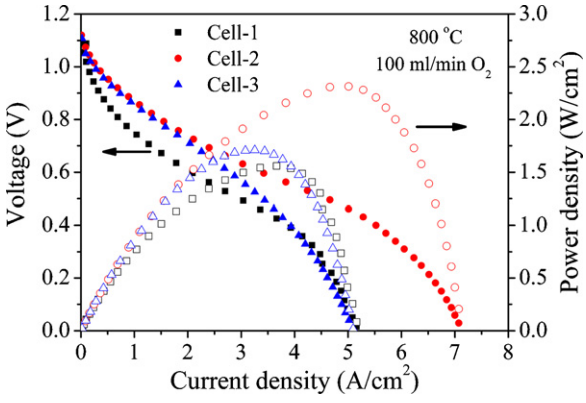

Fig. 5. I–V characteristics of the cells at 800 °C when 100 ml min^{-1} O_2 flow was supplied at the cathode side.

Equation, the slight increase in the OCV means the increase of the oxygen partial pressure and, therefore, the increased oxygen concentration. Obviously, the increase in the OCV is beneficial to boost the cell performance. Furthermore, the increased oxygen concentration facilitates more oxygen molecules to contact the cathode surfaces. And the flowing oxygen can speed up the gas circulation rate within the cathode and expel the nitrogen gas trapped in the inner cathode timely after the exhaustion of the oxygen at high current densities. These factors are helpful for the oxygen dissociative adsorption process in the cathode, which is usually regarded as the rds [21]. Hence, the cell performance is considerably improved due to the increased cathode exchange current density when the oxygen flow is used as the additional oxidant.

At the same time, it is still surprising that such a high increase ratio and such a high cell performance can be obtained by Cell-1 with the pure LSM cathode. The sufficient porosity of the cathode might be the main cause for the fast oxygen circulation rate, resulting in the largely enhanced cathode performance. As mentioned above, the pure LSM in Cell-1 has a larger porosity than the LSM/YSZ in Cell-2, indicating the porosity of the pure LSM cathode is able to supply more sufficient gas flow to support higher current densities for Cell-1 than the LSM/YSZ cathode for Cell-2. However, note that the short-circuit current density of Cell-2 is far larger than that of Cell-1. So the observed negative curvature in the I–V characteristic of Cell-1 should be caused by lack of TPBs for supporting the fast electrochemical reduction reaction at large current densities. The deduction in the present study is in good agreement with another work in our laboratory [22]. By the impregnation of the sufficient SDC loading in the LSM structure, a continuous nano-sized high ion-conducting phase was formed in the surface of LSM network, and the TPBs in the LSM/SDC cathode were far more increased compared with the pure LSM cathode. However, the Cell-3 performance is only 9.6% higher than that of Cell-1, due to the low porosity preventing the fast oxygen transport to and the residual nitrogen out of the active reaction zone. When the oxygen consumption rate is higher than the gas transport rate at a critical current density, the oxygen concentration and, therefore, the oxygen partial pressure is rapidly diminished. It thus leads to the limitation of further promotion of the cell performance mainly due to the serious concentration polarization. Although the porosity of the LSM/YSZ cathode of Cell-2 is somewhat lower than that of the LSM cathode of Cell-1 and the number of cathodic TPB sites of Cell-2 is less than that of Cell-3, the best MPD is still obtained by Cell-2. The pronounced Cell-2 performance is resulted from the combined effects of a rational porosity and a suitable amount of TPBs.

In conclusion, using oxygen as oxidant, a reasonable porosity of the cathode is a most significant factor to achieve a high cell performance. Moreover, possession of another important factor of sufficient amount of TPBs will further promote the cell output considerably.

The relationships between η_e% and current density with the oxygen oxidant are illustrated in Fig. 6. Each curve shows a peak, where the η_e% value is the minimum. The η_e% value of

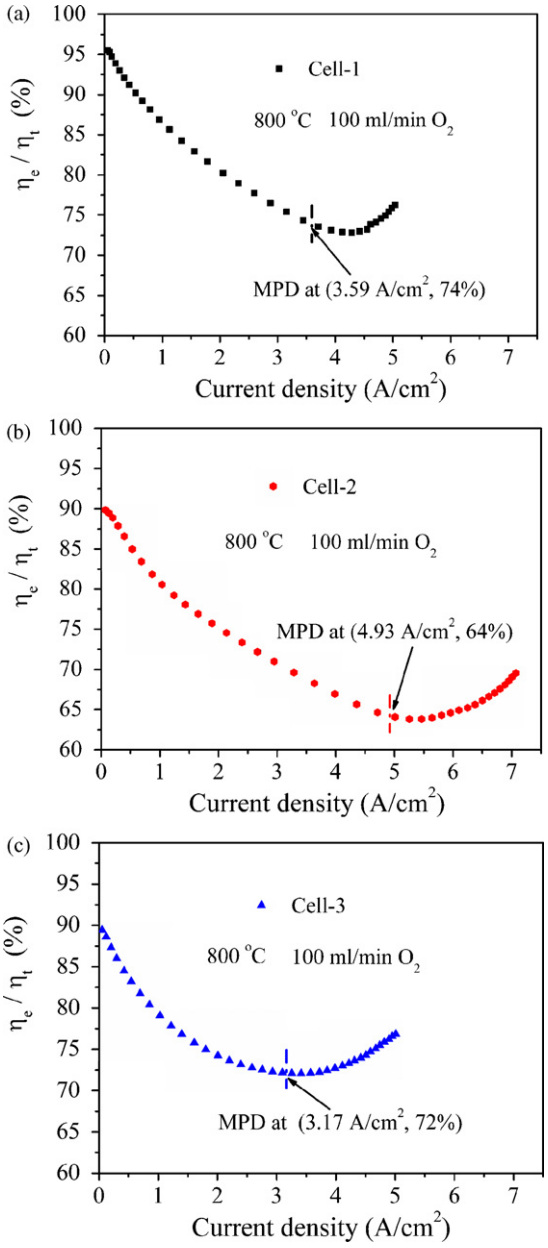

Fig. 6. The ratio of electrode polarization loss in the total cell polarization loss as a function of current density at 800 °C when 100 ml min^{-1} O_2 flow was supplied at the cathode side: (a) Cell-1, (b) Cell-2 and (c) Cell-3.

Cell-3 begins to be bigger than that of Cell-2 when the current density is higher than 2.4 A cm^{-2}, which is due to the dominant cathode concentration polarization. The η_e% values at MPD are 74, 64 and 72% for Cell-1, Cell-2 and Cell-3, respectively. The decrease of the cathode electrode polarization loss results in a significant promotion in the cell performance. As can be seen, along with the decrease in the η_e%, the effect of the ohmic resistance is gradually amplified, which should not be neglected any more. Other than further lowering the YSZ film thickness by decreasing the system reliability, using other ZrO_2-based electrolyte materials with higher conductivities can be an alternative way [23,24].

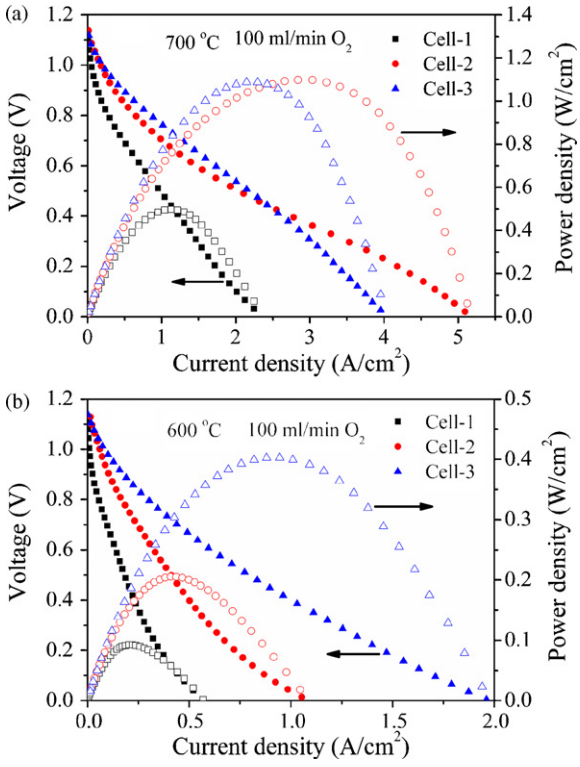

Fig. 7. I–V characteristics of the cells when 100 ml min^{-1} O_2 flow was supplied at the cathode side: (a) at 700 °C and (b) at 600 °C.

3.4. Cell performance at reduced temperatures

Shown in Fig. 7 are the electrochemical characteristics of the cells at 700 and 600 °C with the oxygen oxidant, respectively. The MPD values and the η_e% values at MPD of the three cells at different temperatures are listed in Table 2. As can be seen, the cell performances are all temperature-dependent and decreased rapidly with the reduced temperature, typically for Cell-1. Along with the decrease in the temperature, the output performance of Cell-3 is gradually close to and eventually surpasses that of the Cell-2. The cell performance is eventually dependant on the effect of the amount of TPB length rather than the porosity at reduced temperatures. The concentration polarization due to the low porosity of the LSM/SDC cathode at 800 °C is no longer predominant, since the gas consumption rate is lowered due to relatively low cell output. Under this circumstance, the effect of TPB number on the cathode performance is predominant. As mentioned above, SDC possesses higher ionic conductivity and higher oxygen surface exchange coefficient than YSZ. These advantages in addition to the sufficient TPB sites result

Table 2
MPDs and η_e% values at MPD at varied temperatures

Sample	700 °C		600 °C	
	MPD (W cm^{-2})	η_e% at MPD (%)	MPD (W cm^{-2})	η_e% at MPD (%)
Cell-1	0.50	83	0.09	90
Cell-2	1.10	68	0.21	83
Cell-3	1.09	63	0.40	63

in the enhanced cathode performance, which is responsible for the high output of Cell-3. As can be seen in Table 2, the η_e% values at MPD for both Cell-1 and Cell-2 are increased with the decreased temperature. It means that the cell performance is mainly governed by the electrode polarization loss. In contrast, the η_e% value at MPD for Cell-3 is gradually diminished with the decreased temperature. At the same time, the increasing ohmic polarization loss plays an ever important role in affecting the cell performance with the effective LSM/SDC cathode at reduced temperatures.

So an effective route can be proposed that when a considerable cell output is required at relatively high temperature, e.g., at 800 °C, LSM/YSZ cathode fabricated by the solid mixing method can be adopted, using the oxygen flow as oxidant. On the other hand, LSM/SDC cathode with high SDC weight ratio fabricated by the impregnation process should be employed when a relatively high cell performance is needed at low-to-intermediate temperatures down to 700 °C.

4. Conclusions

The effects of LSM-based cathodes on the cell performance were investigated under various operating conditions. The conclusions were drawn as follows:

1. The cell output was determined by the mutual effects between the gas diffusion rate and TPB length.
2. With the air oxidant, the cell with the LSM/SDC cathode yielded the best MPD at 800 °C.
3. With the oxygen oxidant, the cell with the LSM/YSZ cathode yielded the considerably best MPD at 800 °C.
4. At reduced temperatures down to 700 °C, LSM/SDC cathode was the suitable cathode for zirconia-based electrolyte SOFC.
5. For an excellent cell output, the ohmic polarization loss accounted for a comparable percentage with the cathode polarization loss.

Acknowledgement

The authors gratefully acknowledge the financial supports from the Ministry of Science and Technology of China under contract no. 2001AA323090.

References

[1] N.Q. Minh, Solid State Ionics 174 (2004) 271–277.
[2] Y.H. Zhang, X.Q. Huang, Z. Lu, X.D. Ge, J.H. Xu, X.S. Xin, X.Q. Sha, W.H. Su, Solid State Ionics 177 (2006) 281–287.
[3] K.F. Chen, Z. Lü, N. Ai, X.Q. Huang, Y.H. Zhang, X.D. Ge, X.S. Xin, X.J. Chen, W.H. Su, Solid State Ionics 177 (2007) 3455–3460.
[4] X.S. Xin, Z. Lü, X.Q. Huang, X.Q. Sha, Y.H. Zhang, K.F. Chen, N. Ai, R.B. Zhu, W.H. Su, J. Power Sources 160 (2006) 1221–1224.
[5] T. Tsai, S.A. Barnett, Solid State Ionics 93 (1997) 207–217.
[6] S. de Souza, S.J. Visco, L.C. De Jonghe, Solid State Ionics 98 (1997) 57–61.
[7] S.Z. Wang, Y. Jiang, Y.H. Zhang, J.W. Yan, Solid State Ionics 113–115 (1998) 291–303.
[8] X.Y. Xu, C.R. Xia, G.L. Xiao, D.K. Peng, Solid State Ionics 176 (2005) 1513–1520.
[9] E.P. Murray, Solid State Ionics 143 (2001) 265–273.
[10] S.P. Jiang, W. Wang, Solid State Ionics 176 (2005) 1351–1357.
[11] S.Z. Wang, Y. Jiang, Y.H. Zhang, J.W. Yan, W.Z. Li, J. Electrochem. Soc. 145 (1998) 1932–1939.
[12] J.D. Kim, G.D. Kim, J.W. Moon, Y.I. Park, W.H. Lee, K. Kobayashi, M. Nagai, C.E. Kim, Solid State Ionics 147 (2001) 379–389.
[13] K.F. Chen, Z. Lü, X.J. Chen, N. Ai, X.Q. Huang, W.H. Su, Effect of $La_{0.7}Sr_{0.3}MnO_3$-$Sm_{0.2}Ce_{0.8}O_{1.9}$ cathode on the performance of zirconia film fuel cell, J Funct. Mater., in press.
[14] K.F. Chen, Z. Lü, N. Ai, X.J. Chen, J.Y. Hu, X.Q. Huang, W.H. Su, J. Power Sources 167 (2007) 84–89.
[15] Y. Jiang, S. Wang, Y. Zhang, J. Yan, W. Li, J. Electrochem. Soc. 145 (1998) 373–378.
[16] P. Charpentier, P. Fragnaud, D.M. Schleich, E. Gehain, Solid State Ionics 135 (2000) 373–380.
[17] Y.L. Zhang, J.F. Gao, D.K. Peng, G.Y. Meng, X.Q. Liu, Ceram. Int. 30 (2004) 1049–1053.
[18] K. Eguchi, J. Alloys Compd. 250 (1997) 486–491.
[19] Z.W. Wang, M.J. Cheng, Y.L. Dong, M. Zhang, H.M. Zhang, Solid State Ionics 176 (2005) 2555–2561.
[20] Y.J. Leng, S.H. Chan, K.A. Khor, S.P. Jiang, Int. J. Hydrogen Energy 29 (2004) 1025–1033.
[21] E.P. Murray, T. Tsai, S.A. Barnett, Solid State Ionics 110 (1998) 235–243.
[22] N. Ai, Z. Lü, K.F. Chen, X.Q. Huang, X.B. Du, W.H. Su, Effects of anode surface modification on the performance of low temperature SOFCs, J. Power Sources, submitted for publication.
[23] Z.W. Wang, M.J. Cheng, Y.L. Dong, M. Zhang, H.M. Zhang, J. Power Sources 156 (2006) 306–310.
[24] K. Yamahara, C.P. Jacobson, S.J. Visco, X.F. Zhang, L.C. De Jonghe, Solid State Ionics 176 (2005) 275–279.